PCCP

This is an *Accepted Manuscript*, which has been through the Royal Society of Chemistry peer review process and has been accepted for publication.

Accepted Manuscripts are published online shortly after acceptance, before technical editing, formatting and proof reading. Using this free service, authors can make their results available to the community, in citable form, before we publish the edited article. We will replace this *Accepted Manuscript* with the edited and formatted *Advance Article* as soon as it is available.

You can find more information about *Accepted Manuscripts* in the **Information for Authors**.

Please note that technical editing may introduce minor changes to the text and/or graphics, which may alter content. The journal's standard **Terms & Conditions** and the **Ethical guidelines** still apply. In no event shall the Royal Society of Chemistry be held responsible for any errors or omissions in this *Accepted Manuscript* or any consequences arising from the use of any information it contains.

Physical Chemistry Chemical Physics

Paper

Electron transport characteristics in nano-segregated columnar phases of perylene tetracarboxylic bisimide derivatives bearing oligosiloxane chains

Masahiro Funahashi,*[a] and Akinari Sonoda[b]

Electron transport characteristics in nanosegregated columnar phases of perylene tetracarboxylic bisimide (PTCBI) derivatives bearing oligosiloxane chains are studied over wide temperature ranges using a time-of-flight (TOF) method. In the ordered columnar phases of the PTCBI derivatives bearing disiloxane chains, the electron mobilities exceed 0.1 $cm^2V^{-1}s^{-1}$ at room temperature. In the disordered columnar phase of the PTCBI derivative bearing trisiloxane chains, the electron mobility reaches the order of 10^{-3} $cm^2V^{-1}s^{-1}$ around room temperature. These electron mobilities are temperature-independent around room temperature. However, their dependence upon the electric field becomes larger when the temperature is lowered below room temperature; this behavior is described by a hopping transport mechanism. The experimental results are analyzed using a one-dimensional disorder model.

Introduction

Solution-processable organic semiconductors have the potential to completely transform production processes of electronic devices such as light emitting diodes (LEDs), field-effect transistors (FETs), and solar cells.[1] In the future, various electronic devices will be produced by printing methods such as ink-jet and roll-to-roll processes,[2] although, at present, most organic electronic devices are fabricated by vacuum processes.

High solubilities of the organic semiconductors in organic solvents are required for the production of organic electronic devices by printing technologies. In general, alkyl chains are introduced to the aromatic cores of organic semiconductor molecules in order to increase their solubilities. However, bulky alkyl chains often inhibit close molecular packing and lower their carrier mobilities.[3]

Liquid crystalline (LC) semiconductor molecules consist of alkyl chains appended to an extended π-conjugated core associated with electronic charge carrier transport; the alkyl chains function to induce solubility in organic solvents. Efficient electronic charge-carrier transport phenomena have been observed in columnar,[4] nematic,[5] and smectic phases.[6] Furthermore, some LC semiconductors are also solution-processable. LEDs emitting linearly polarized light were fabricated using LC semiconductors.[7] Columnar and smectic LC semiconductors have also been applied to FETs[8] and solar cells.[9] LC semiconductors have the advantages of flexibility and softness over molecular crystals. Flexible FETs based on LC phenylterthiophene have been reported.[8d] However, the number of reported LC semiconductors exhibiting high carrier mobility as well as solution-processability has been limited because the extended π-conjugated moieties cause low solubility and crystallization, resulting in the formation of inhomogeneous films with a high density of defects.

Another advantage of LC semiconductors is the formation of superstructures based on the nanosegregation.[10] LC molecules consisting of incompatible parts exhibit various nanosegregated mesophases including layer, columnar, micellar cubic, and bicontinuous cubic phases.[10e,f,g] LC phenylterthiophene derivatives bearing an imidazolium moiety exhibit nanostructured smectic phases for alternately integrated ion-conductive and hole-conductive layers, resulting in electrochromism without electrolyte solutions.[10h,i]

We have closely examined oligosiloxane moieties as side-chains of LC molecules[11] and recently reported LC perylene tetracarboxylic bisimide (PTCBI) derivatives bearing oligosiloxane chains.[12] The electron mobility of an LC-PTCBI derivative exceeds 0.1 $cm^2V^{-1}s^{-1}$ at room temperature.[12b] Because of thermal motions of the oligosiloxane chains, the PTCBI derivatives exhibit high solubility in organic solvents except for alcohols, and their thin films can be produced by a spin-coating method.[12a,b] In spite of the large aromatic cores

giving rise to strong π–π interactions, these derivatives exhibit columnar phases at room temperature and do not crystallize even when cooled to −100 °C. Nanosegregation between the aromatic cores and oligosiloxane chains plays a significant role during formation of the columnar phases.[12c,d] One-dimensional aggregates of π-conjugated cores in the columnar phases of the PTCBI derivatives, over which electrons are transported, are surrounded by liquid-like mantles, resulting in efficient electron transport properties and improved solubility as well as flexibility.

In this study, the electron mobilities in the columnar phases of PTCBI derivatives bearing oligosiloxane chains are measured over wide temperature ranges using a time-of-flight (TOF) technique. Analysis of the electron transport characteristics in the columnar phases based on a one-dimensional disorder model[13] reveals the hopping nature of the electron transport in the nanosegregated columnar phases.

Theoretical models based on the dependence of the transfer integral on azimuthal angles of the LC molecules within the columnar aggregates have been reported; these models provide an effective strategy for the molecular design of new columnar LC semiconductors.[14] In order to understand the influence of molecular aggregation states on the carrier transport characteristics, analysis of the dependence of carrier mobility on the electric field and temperature is required. Up to now, studies based on Gaussian disorder[13] and small polaron hopping models[15] have been reported for few columnar LC phases.[16] Measurement of carrier mobility over wide temperature and electric field ranges is necessary to estimate the disorder parameters; however, the mesomorphic temperature ranges of LC semiconductors are generally only several tens of degrees, making it difficult to ascertain the parameters with any precision. The extremely wide temperature ranges exhibited by the LC-PTCBI derivatives bearing oligosiloxane chains make it possible to study their electron transport mechanism; accordingly, this research is anticipated to enhance our mechanistic understanding and to improve the carrier transport properties of LC semiconductors in the design of new materials.

Experimental

Materials

Scheme 1 shows the molecular structures of LC-PTCBI derivatives **1–3** bearing four disiloxane or four trisiloxane chains used in this study. The synthetic procedures and mesomorphic properties of compounds **1** and **3** have been reported previously.[12a,b] The synthetic procedures and spectral data for compound **2** are described in the Supporting Information. The PTCBI derivatives were purified by silica gel column chromatography. The crude products were then dissolved in dichloromethane and the resulting solutions were poured into methanol. The produced precipitates were filtered and dried under vacuum. Their mesomorphic properties were studied using differential scanning calorimetry (DSC), polarizing optical microscopy, and X-ray diffraction. Detailed

data of morphologial studies are provided in the Supporting Information.
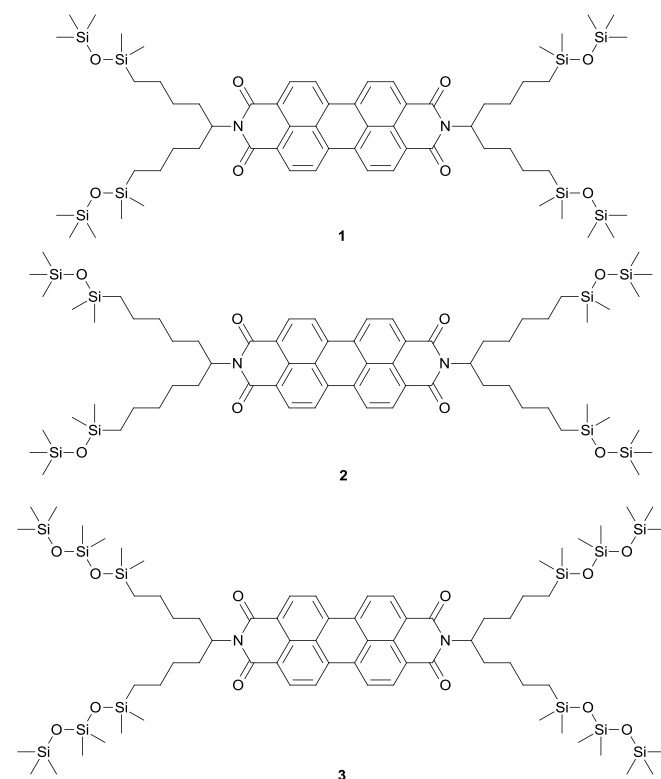
Scheme 1 Molecular structures of PTCBI derivatives **1–3** bearing four oligosiloxane chains.

Mesomorphic properties of PTCBI derivatives 1-3

The phase transition temperatures of compounds **1–3** are summarized in Table 1. All of the compounds exhibit columnar phases and do not crystallize even upon cooling to −100 °C. Compounds **1** and **2** bearing disiloxane chains exhibit ordered columnar phases at room temperature. In the ordered columnar phases, the LC molecules stack periodically within the columnar aggregates and exhibit an intermolecular distance within the columns of around 3.5 Å. This value indicates the existence of a π–π stacking interaction in the LC columnar aggregates. Compound **1** exhibits hexagonal and rectangular ordered columnar phases,[12b] while compound **2** shows a single hexagonal ordered columnar phase (see Supporting Information).

Table 1 Phase transition temperatures and enthalpies of the PTCBI derivatives.

	Phase transition temperature/ °C [enthalpy/Jg⁻¹]
Compound **1**	heating: G −56.0 Col_{ro} 47.0 [1.9] Col_{ho} 138.3 [6.2] Iso cooling: G −56.0 Col_{ro} 32.4 [1.4] Col_{ho} 135.3 [6.0] Iso
Compound **2**	heating: G −54.0 Col_{ho} 129.0 [4.8] Iso cooling: G −59.0 Col_{ho} 125.6 [4.6] Iso
Compound **3**	heating: G −82 Col_{hd} 50.5 [2.7] Iso cooling: G −86 Col_{hd} 50.5 [2.7] Iso

Col_{ro}: columnar rectangular ordered phase; Col_{ho}: columnar hexagonal ordered phase; Col_{hd}: columnar hexagonal disordered phase; G: glassy columnar phase

2 | *Phys. Chem. Phys. Chem.*, 2014, **00**, 1-3

This journal is © The Royal Society of Chemistry 2012

In contrast, the structure of the columnar phase of compound **3** is disordered and has no periodical order in the molecular positions within the columnar aggregates. Moreover, the hexagonal arrangement is also ambiguous.[12a]

All of the compounds exhibit glass transitions, which are attributed to the frozen liquid-like motion of oligosiloxane chains. These compounds are waxy and soft at room temperature, which can be explained by the thermal motions of the oligosiloxane chains.

Determination of the electron mobilities in the columnar phases

The electron mobilities in the columnar phases of the PTCBI derivatives **1**–**3** were measured by the TOF method.[17] The PTCBI derivatives were melted to obtain isotropic liquids, which were capillary-filled into cells consisting of two ITO-coated glass plates on a hot plate. The LC cell was placed on a hot stage with a PID thermocontroller. For measurements below room temperature, a cryostat (Oxford Optistat) was used.

The cell was illuminated by a laser pulse, and an induced photocurrent was recorded in a digital oscilloscope (Tektronix TDS3044B) through a serial resistor. The third harmonic generation of a Nd:YAG laser (Continuum, Minilite II, wavelength = 355 nm, pulse duration = 2 ns) was used as an excitation source.

Carriers are generated at the interface between the illuminated electrode and LC bulk by pulse excitation. The photo-generated carriers drift across the sample, thereby inducing a displacement current in the serial resistor; the transient photocurrent decays when the carriers arrive at the counter electrode. Transit time (t_T), in which the photo-generated carriers are transported through the bulk of the sample, is determined from a kink point in the transient photocurrent curve. Electron mobility (μ) can be determined when the illuminated electrode is negatively biased using Equation 1, where V and d are applied voltage and sample thickness, respectively.

$$\mu = \frac{d^2}{V t_T} \qquad (1)$$

In the TOF measurement of columnar LC phases, the orientation control of the columnar axes of the LC materials is significant because the carrier transport is one-dimensional and the mobility along the columnar axis is several orders of magnitude higher than that perpendicular to the axis.[4a,c,j] In this study, we could not obtain a sufficiently strong signal to determine the transit times of the photogenerated charge carriers when homogeneously aligned samples were used. In order to achieve the homeotropical alignment of columnar aggregates, hydrophilic surface treatment is necessary.

The samples in which columnar aggregates are homeotropically aligned were prepared as follows. The surfaces of patterned ITO-coated glass plates were cleaned by a UV–ozone treatment. The resulting substrates were dipped in a toluene solution of 3-aminopropyl triethoxysilane (5 wt%) for 24 h. During this process, the electrode surfaces became

hydrophilic. A measurement cell was fabricated by adhering the two substrates with glue using polyethylene film spacers.

Carrier transport model in one-dimensional columnar aggregates

The Gaussian disorder model regarding electronic charge carrier transport in disordered systems, including organic amorphous glasses, has been proposed by Bässler.[18] In this model, electronic charge carrier movement is described as a charge-carrier hopping process between energy levels in a Gaussian density of states (DOS) distribution. Photogenerated charge carriers are thermally relaxed in the Gaussian DOS; excitation of these relaxed charge carriers to a transport level located at the centre of the DOS is the rate-determining process during carrier transport. This excitation is assisted by heat and the electric field, resulting in the temperature- and field-dependence of carrier mobilities. By means of a Monte Carlo simulation, Bässler *et al.* obtained the relationships between the carrier mobility, μ, temperature, T, and electric field, F, as described in Equations 2 and 3:

$$\mu = \mu_0 \exp\left[-\left(\alpha \frac{\sigma}{k_B T}\right)^2\right] \exp\left[C\left\{\left(\frac{\sigma}{k_B T}\right)^2 - \Sigma^2\right\}\sqrt{F}\right] \quad \Sigma \geq 1.5 \quad (2)$$

$$\mu = \mu_0 \exp\left[-\left(\alpha \frac{\sigma}{k_B T}\right)^2\right] \exp\left[C\left\{\left(\frac{\sigma}{k_B T}\right)^2 - 2.25\right\}\sqrt{F}\right] \quad \Sigma \leq 1.5 \quad (3)$$

The disorder parameters σ and Σ indicate the width of the Gaussian DOS and the dimensionless value for distribution of the intermolecular transfer integrals, respectively; parameter μ_0 is a pre-exponential factor related to the transfer integral; parameter C is a constant having a dimension of $V^{-1/2}cm^{1/2}$, and; k_B is the Boltzmann constant. In a conventional Gaussian disorder model, three-dimensional migration of charge carriers is assumed and parameter α is 2/3.[18]

In one-dimensional systems, the thermal relaxation process exhibited by charge carriers is different from that of three-dimensional systems. In a one-dimensional system, carriers can move only forward or backward, while avoiding deep levels and defects in two- and three-dimensional systems. According to the model proposed by Bleyl and Haarer,[14a] carrier mobility, μ, is described as Equation 4:

$$\mu = \mu_0 \exp\left[-\left(0.9 \frac{\sigma}{k_B T}\right)^2\right] \exp\left[C\left\{\frac{\sigma}{k_B T} - \Sigma\right\}\sqrt{F}\right] \qquad (4)$$

In this study, the results of temperature- and field-variable TOF measurements in the columnar phases of PTCBI derivatives **1**–**3** were analyzed based on Equation 4. At $F = 0$, Equation 4 can be further simplified as shown in Equation 5:

$$\mu(F = 0) = \mu_0 \exp\left[-\left(0.9 \frac{\sigma}{k_B T}\right)^2\right] \qquad (5)$$

The zero-field mobility, $\mu(F = 0)$, can be determined by an extrapolation of the measured mobility values to the zero-field in a plot of mobility *vs.* the square root of the electric field.

Therefore pre-exponential factor μ_0 and energetic disorder σ can be derived from the intercept and slope value of the plot of the logarithm of μ $(F = 0)$ *vs.* $(1/k_B T)^2$.

The field-dependence of electron mobility β is expressed as Equation 6:

$$\beta = \frac{\partial \log \mu}{\partial \sqrt{F}} = C \left(\frac{\sigma}{k_B T} - \Sigma \right) \qquad (6)$$

β is determined from a plot of the logarithm of electron mobility *vs.* the square root of the electric field; parameters C and Σ are obtained from a plot of β *vs.* $1/k_B T$.

Results and Discussion

Orientation control of the columnar aggregates

Figure 1 shows polarizing micrographs of the columnar phases of PTCBI derivatives **1–3**. In contrast to the samples prepared using non-treated cells, dark-field domains are observed in the LC cells of which electrode surfaces were treated to be hydrophilic, indicating homeotropic alignment of the columnar aggregate. For compounds **1** and **2**, defect lines are formed at room temperature due to shrinkage of the two-dimensional lattices.
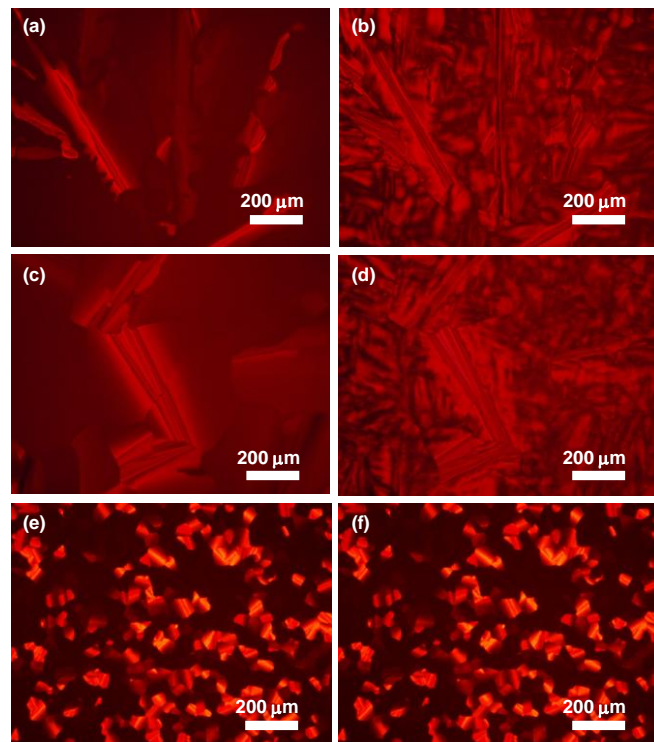

Figure 1 Polarizing micrographs of homeotropically aligned samples of the columnar phases of compound **1** at (a) 120 °C and (b) 30 °C, compound **2** at (c) 120 °C and (d) 30 °C, and compound **3** at (e) 50 °C and (f) 30 °C.

Electron transport in the columnar phases of compounds 1–3

Figures 2(a)–(c) exhibit the transient photocurrent curves in the columnar phases of compounds **1–3** at room temperature. Above 220 K, non-dispersive transient photocurrent curves

were obtained in all columnar phases of these compounds and transit times were clearly determined. Below this temperature, the photocurrent signals became weak and dispersive. In these low temperature regions, the electron mobilities could not be determined.
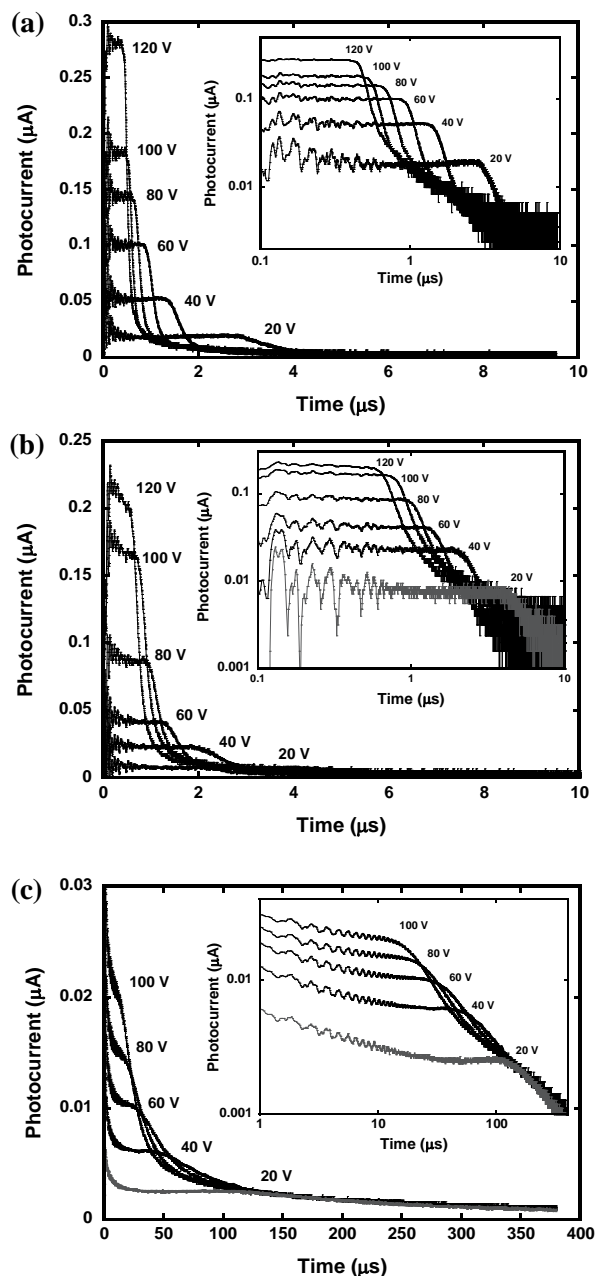

Figure 2 Transient photocurrent curves for electrons at 300 K in the columnar phases of (a) compound **1** (d = 27 μm), (b) compound **2** (d = 25 μm), and (c) compound **3** (d = 15 μm). The insets are double logarithmic plots of the photocurrent curves.

Figure 3 illustrates the electron mobilities in the columnar phases of compounds **1–3** as a function of temperature under a electric field of 5×10^4 Vcm^{-1}. The electron mobilities of compounds **1** and **2** decrease with an increase in temperature above 300 K and 350 K, respectively. In contrast, mobilities

increase at a temperature below 270 K for compound **1** and below 320 K for compound **2**; between these two temperature ranges, the electron mobilities are temperature-independent for both compounds. In the disordered columnar phase of compound **3**, electron mobility decreases monotonically with a decrease in temperature. In addition, the temperature-dependence of the mobility becomes remarkable below 270 K.
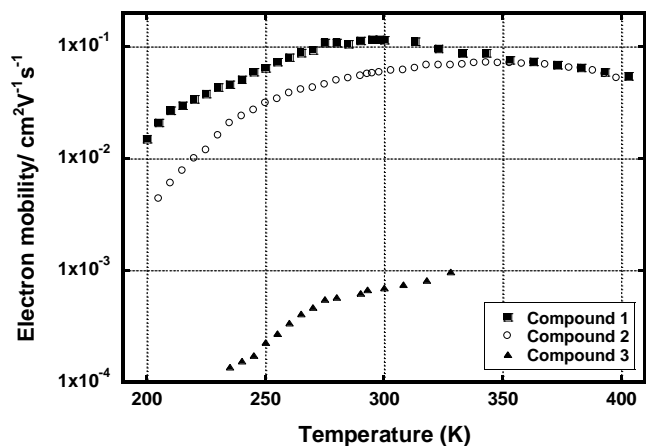

Figure 3 Electron mobilities in the columnar phases of compounds **1–3** at the electric field of 5 x 10^4 Vcm^{-1} as a function of temperature.

Electron transport processes in the columnar phases of compounds 1–3 in high-temperature regions

Figure 4 displays X-ray diffraction patterns of the columnar phases of compounds **1** and **2** in a wide-angle region at various temperatures. The full-range X-ray diffraction patterns of compounds **1–3** are provided in the Supporting Information. The peaks in the patterns are located around $2\theta = 25°$ and the corresponding lattice constants are about 3.5 Å; these values indicate the existence of a $\pi-\pi$ stacking interaction between the LC molecules and allude to a periodicity in the intermolecular distances within the columnar aggregates of these compounds. In contrast, the columnar phase of compound **3** shows no periodical order within the columnar aggregates, and its two-dimensional columnar arrangement is also disordered.

Figure 5 shows the $\pi-\pi$ stacking distance within the columnar aggregates in the columnar phases of compounds **1** and **2**. For compound **1**, the $\pi-\pi$ stacking distance decreases with an increase in temperature in the hexagonal ordered columnar phase above 40 °C. In the rectangular ordered columnar phase below 40 °C, the distance remains constant. For compound **2**, the $\pi-\pi$ stacking distance decreases gradually with a decrease in temperature above 50 °C. Below 50 °C, the distance is independent of temperature. However, the decrease in distance is more remarkable for the hexagonal ordered columnar phase of compound **1** than for that of compound **2**. This shrinkage can be attributed to a pre-transitional effect for the phase transition from the hexagonal to rectangular columnar phase.
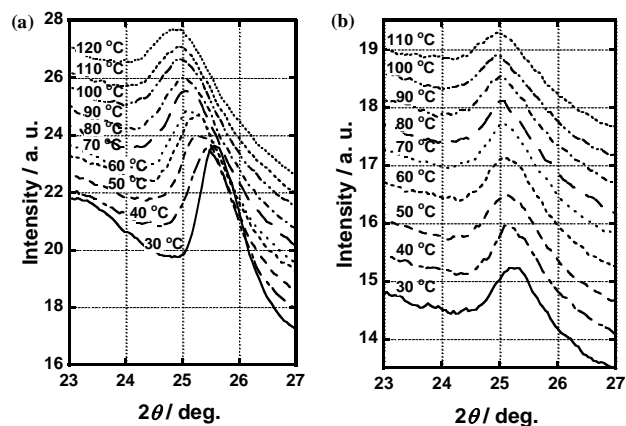

Figure 4 X-ray diffraction patterns in the wide-angle region in the columnar phases of (a) compound **1** and (b) compound **2**.
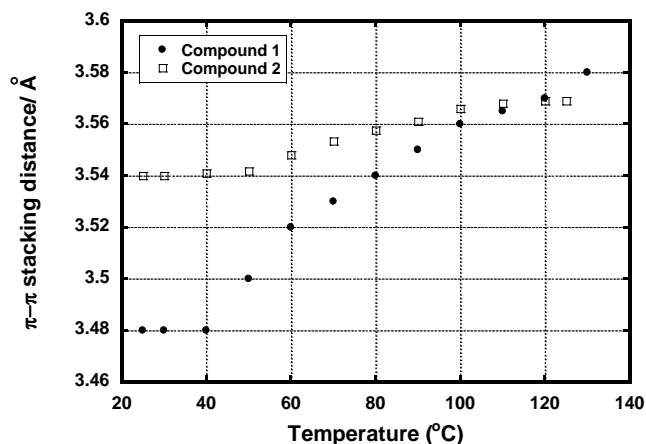

Figure 5 $\pi-\pi$ stacking distance in the columnar phases of compounds **1** and **2** as a function of temperature.

As shown in Figure 3, for compound **1**, electron mobility increases from 5.4×10^{-2} to 1.1×10^{-1} cm^{2}V^{-1}s^{-1} when the temperature is decreased from 410 to 310 K. However, for compound **2**, electron mobility increases only slightly from 5.2×10^{-2} to 6.9×10^{-2} cm^{2}V^{-1}s^{-1} in the narrow temperature range from 397 to 370 K. In these temperature ranges, the electron mobilities are field-independent.

These increases in electron mobility in the hexagonal columnar phases of compounds **1** and **2** may be attributed to the observed shrinkage of $\pi-\pi$ stacking distances within the columnar aggregates. The shrinkage is caused by a decrease in the thermal fluctuation of the columnar structures of these compounds. Compound **1** exhibits a more ordered structure at room temperature compared to compound **2**, and the columnar aggregate shrinkage of compound **1** should be more remarkable than that of compound **2**.

Around room temperature, the electron mobilities of compounds **1** and **2** are independent of temperature. As mentioned in the next section, the electron transport mechanism below room temperature involves one-dimensional charge carrier hopping, which is a thermal- and field-activation process.

This journal is © The Royal Society of Chemistry 2012

Phys. Chem. Chem. Phys., 2014, **00**, 1-3 | **5**

Therefore, the effects of expanding the π–π stacking distance caused by thermal fluctuations should cancel the thermal activation effect in the charge-carrier hopping transport process, producing temperature-independent electron mobility around room temperature.

In the columnar phase of compound **3**, the electron mobility shows dependence on both the electric field and temperature. However, this dependence decreases above 270 K. This also should be attributed to the cancellation of these two effects.

Electron transport processes in the columnar phases of compounds 1 and 3 in low-temperature regions

In spite of electron mobility distributions between the orders of 10^{-1} and 10^{-4} cm^{2}V^{-1}s^{-1} at room temperature among compounds **1**–**3**, the temperature- and field-dependences of electron mobilities in the columnar phases of these compounds are similar below room temperature.

Figures 6(a)–(c) exhibit electron mobilities below room temperature as a function of the square root of the electric field at various temperatures. For all compounds (**1**–**3**), the logarithms of the electron mobilities are proportional to the square root of the electric field below room temperature, although data points are scattered slightly below 220 K. The slopes (β) in the plots increase with a decrease in the temperatures for these compounds. This behavior is similar to conventional organic amorphous semiconductors containing energetic and spatial disorders, although the electron mobilities in the ordered columnar phases of compounds **1** and **2** are much higher than those of organic amorphous semiconductors.

The electron transport characteristics in the columnar phases of compounds **1**–**3** indicates the hopping nature of electron transport, which is quite different from that of band conduction in which carrier mobility is independent of temperature or exhibits a negative temperature dependence due to phonon scattering.[19]

The carrier transport process in organic amorphous semiconductors can be described by a three-dimensional Gaussian disorder model.[18] The process in the case of electron transport in the columnar phases is one-dimensional because the electrons are transported through the orbital overlaps between π-conjugated cores located at the columnar aggregate centers, while the electron transport paths are separated by the insulative alkyl and siloxane chains. In fact, strong photocurrent signals are observed in the homeotropically aligned samples, while weak featureless photocurrent decays are obtained in homogeneous aligned samples in which columnar axes are perpendicular to the electric field. Therefore, the electron transport characteristics in the low temperature regions for these PTCBI derivatives **1**–**3** can be analyzed based on the one-dimensional disorder model proposed by Bleyl and Haarer.[13a] The experimentally obtained data between room temperature and 220 K were used for this analysis.
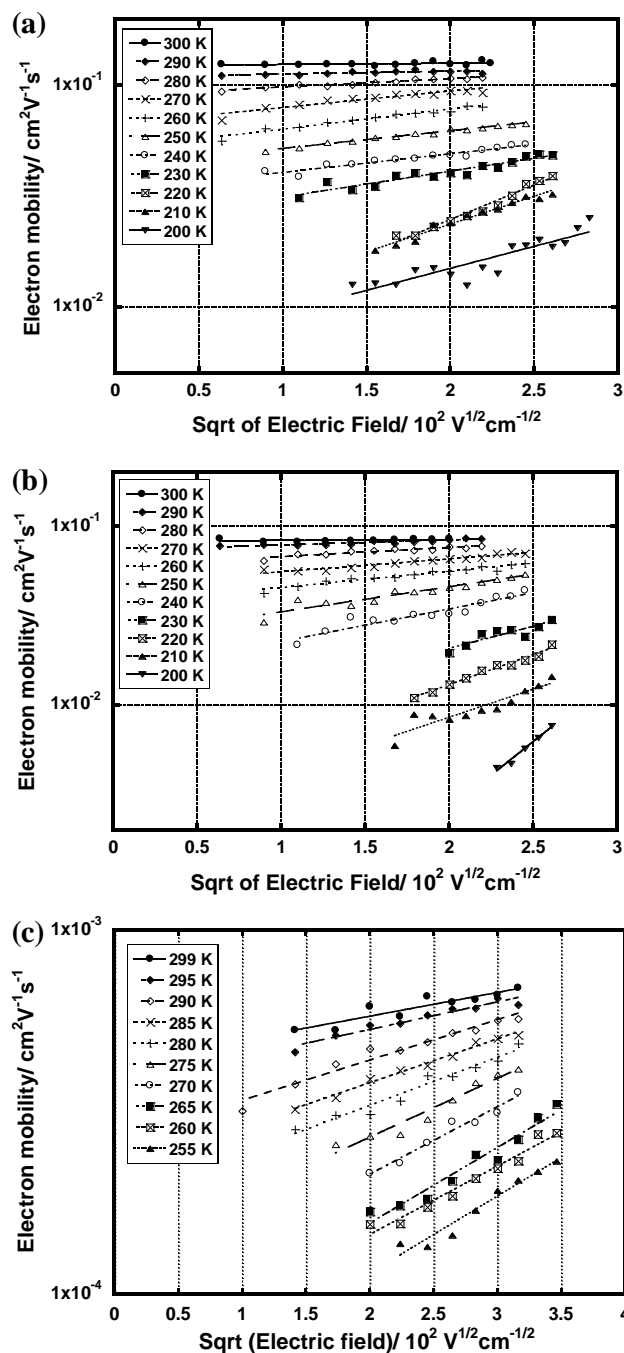

Figure 6 Electron mobility as a function of the electric field at various temperatures below 300 K for (a) compound **1**, (b) compound **2**, and (c) compound **3**.

Figure 7(a) illustrates the zero-field electron mobility below room temperature for compounds **1**–**3** as a function of $1/(k_BT)^2$. Above 220 K, the zero-field mobilities were proportional to $1/(k_BT)^2$. Parameters μ_0 and σ could thus be calculated based on Equation (4). Figure 7(b) shows the field-dependence of electron mobilities (β) below room temperature as a function of $1/k_BT$. For all compounds, the experimental data show good fitting with the theoretical equation as shown in Figure 7 although the data tend to scatter below 220 K. The fittings were

carried out using experimental data above 220 K. The slopes of the fitted lines are $C\sigma$ and the intercepts are $C\Sigma$. The calculated disorder parameters are summarized in Table 2.
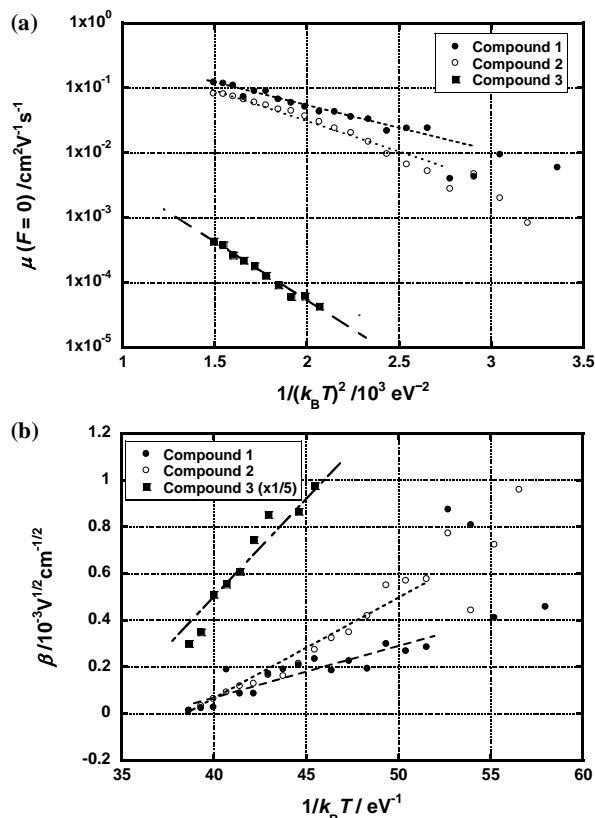

Figure 7 (a) Electron mobilities at zero-field as a function of $1/(k_BT)^2$ for the columnar phases of compounds **1–3**. (b) Field-dependence of the electron mobilities, β, as a function of $1/k_BT$.

The values of μ_0 for compounds **1** and **2** exceed 1 cm^{2}V^{-1}s^{-1} while μ_0 is on the order of 10^{-1} cm^{2}V^{-1}s^{-1} for compound **3**. These values are also much higher than those of organic amorphous semiconductors. The columnar phases of compounds **1** and **2** are ordered such that periodical $\pi-\pi$ stacking structures exist in their columnar aggregates. These greater values of μ_0 for compounds **1** and **2** can be attributed to larger transfer integrals. For compound **3**, the absence of periodical stacking order within the columnar structure results in a smaller value of μ_0.

The distribution widths of the DOS (σ) are 43 and 52 meV for the rectangular ordered columnar phase of compound **1** and hexagonal ordered columnar phase of compound **2**, respectively. The rectangular ordered phase usually appears in a lower temperature range and has a more ordered structure than that of the hexagonal ordered phase. The smaller value of σ in the rectangular ordered columnar phase of compound **1** than that in the hexagonal ordered columnar phase of compound **2** is reasonable. In contrast, the value of σ increases to 72 eV in the disordered columnar phase of compound **3**, which is attributed to the disordered structure of the columnar phase of compound **3**.

Parameter Σ also exhibits the same tendency as the values of σ. The disordered columnar phase of compound **3**, which has the most disordered structure, exhibits the largest Σ. For compounds **1** and **2**, the longer the alkylene spacers present, the greater the disorder parameters σ and Σ become. Thermal fluctuation and freedom of conformation of the oligosiloxane chains should have an influence on the packing of π-conjugated cores. In the case of compound **3**, this effect perturbs the one-dimensional closed molecular packing structure, resulting in the appearance of the disordered columnar phase.

Table 2 Disorder parameters in the columnar phases of compounds **1–3**.

	μ_0 (cm^{2}V^{-1}s^{-1})	σ (meV)	Σ	C (cm$^{1/2}$V$^{-1/2}$)
Compound **1**	1.20	43	1.57	4.7×10^{-4}
Compound **2**	2.49	52	1.94	8.0×10^{-4}
Compound **3**	2.15×10^{-1}	72	2.54	7.2×10^{-3}

Comparison with other LC semiconductors

Up to now, the carrier transport mechanism has been studied for few LC semiconductors because of the scarcity of such materials exhibiting LC phases over wide temperature regions. Scheme 2 illustrates LC semiconductors in which the disorder parameters are estimated using the one-dimensional disorder formalism.[13a] The obtained disorder parameters for compounds **4–6** are summarized in Table 3.
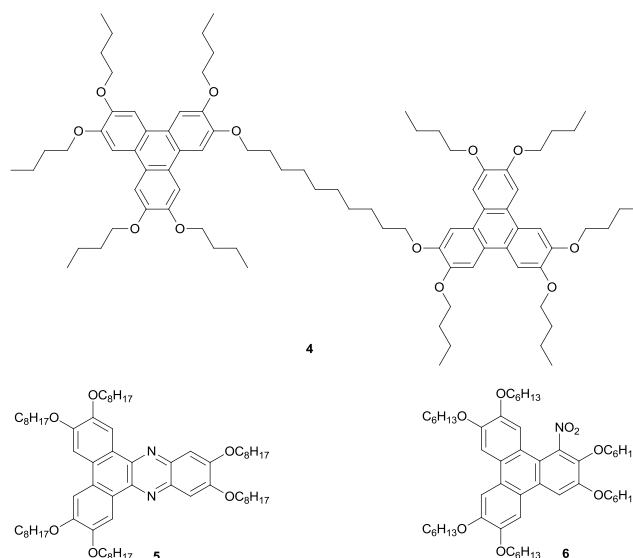
Scheme 2 Molecular structures of columnar liquid crystals whose carrier transport characteristics were analyzed by the Gaussian disorder model.

The values of σ in the ordered columnar phases of compounds **1** and **2** are 40–50 meV; these values are comparable to that in the discotic plastic phase of triphenylene dimer **4** as reported by Bleyl and Haarer.[13a] This discotic plastic phase is a hexagonal ordered columnar phase in the recent terminology and has a periodical $\pi-\pi$ stacking structure in the columnar aggregates. It should be noted that the difference in the electron transport characteristics between the PTCBI

ARTICLE

derivatives and the triphenylene dimer is in the value of μ_0 rather than σ. Parameter σ is the width of the distribution of LUMO levels, which is caused by a disorder in the local electric field. The disorders of the ordered columnar phase of compounds **1–2** and the triphenylene dimer discotic plastic phase are not so different. In contrast, parameter μ_0 is strongly dependent upon the transfer integral between adjacent π-conjugated cores in the columnar aggregates. The transfer integral can be changed by extension of the π-conjugated cores, $\pi-\pi$ stacking distances, and azimuthal angles between the adjacent molecules.

Compound **5** exhibits ambipolar carrier transport properties, although its columnar phase does not have such a closed packing structure as those exhibited by compounds **1** and **2**. The pre-exponential factor (μ_0) of compound **5** is two orders of magnitude smaller than those of compounds **1** and **2**. As Iino described for compound **6**, the parameter σ is strongly influenced by the dipole moment of LC molecules.[13b] In the columnar phase of compound **6**, the large values of σ for the holes and electrons can be attributed to the disordered structure of the columnar aggregates as well as the polar aromatic core.

Compared to the columnar LC compounds **4–6**, compounds **1–3** having oligosiloxane chains exhibit a prominent feature in their carrier transport properties; it should be noted that the disiloxane chains of compounds **1** and **2** do not increase the disorder parameter σ as well as Σ, and do not decrease μ_0 in spite of their bulkiness and liquid-like disordered conformation. Since the disiloxane chains are separated from the π-conjugated cores, they do not exert an influence on the packing structure of the PTCBI moieties. In the columnar phases of compounds **1** and **2**, the electron-transporting one-dimensional stacking structure surrounded by the insulative oligosiloxane mantle is formed by nanosegregation. The stacking structure is rigid, while the mantle consisting of oligosiloxane chains is soft and flexible. This nanosegregated hybrid structure provides a flexible material with efficient electron transport properties.

Table 3 Disorder parameters in other columnar LC semiconductors.

	μ_0 (cm^{2}V^{-1}s^{-1})	σ (meV)	Σ	C (cm$^{1/2}$V$^{-1/2}$)
Compound **4**	0.25	48	2.4	5.7×10^{-3}
Compound **5**	2.1×10^{-2} (hole)	62	---	---
	8.2×10^{-2} (electron)	70	---	---
Compound **6**	0.86	102	---	---

For compounds **5** and **6**, Σ and C are not shown.

Carrier transport characteristics in the smectic phases of terthiophene derivatives have been studied using the TOF method. Hole mobilities were measured in wide temperature ranges for the smectic B hexatic, B crystal, and E phases of cyclohexylethylterthiophene[16c] and alkynylterthiophene[16b] derivatives, and their disorder parameters were determined based on a two-dimensional Gaussian disorder model. The value σ does not strongly depend upon the LC molecular aggregation states; accordingly, the value is around 50 meV in these smectic phases. The molecular aggregation states have influence on the parameter μ_0 rather than σ and Σ.

TOF measurements of the nematic phase of a photo-polymerized fluorene derivative revealed temperature- and field-dependent hole mobility below room temperature. Based on the three-dimensional Gaussian and correlation disorder models,[18a,d] a σ value of 89 meV was obtained. In the nematic phase, molecular aggregation is loose and disordered; as a result, the hole transport mechanism is similar to that of amorphous organic semiconductors.

In the ordered columnar phases of LC-PTCBI derivatives **1** and **2**, the electron mobilities at room temperature are comparable to those of molecular crystals. In particular, mobility exceeds 0.1 cm^{2}V^{-1}s^{-1} in the rectangular ordered columnar phase of compound **1** at room temperature. This value is comparable to that in an ordered smectic phase of the LC phenylterthiophene derivative.[16a] However, the carrier transport mechanism is quite different between these two systems. In contrast to the band-like hole transport in the smectic phase of the phenylterthiophene derivative, charge carrier hopping is a predominant process in the ordered columnar phases of PTCBI derivatives in this study. At present, we are unable to conclude the reason for this; one possible explanation is that the one-dimensional system is strongly influenced by localized states and defects. The carriers can move only forward or backward and cannot escape from a defect in one-dimensional electronic systems, while they can move avoiding the traps in two-dimensional systems.

Conclusions

Electron transport characteristics in nano-segregated columnar phases of perylene tetracarboxylic bisimide (PTCBI) derivatives bearing oligosiloxane chains have been studied over wide temperature ranges using a time-of-flight (TOF) method. For ordered columnar phases of compounds **1** and **2**, the electron transport process is influenced by thermal fluctuations of the columnar aggregates in high-temperature regions. In the low-temperature regions of the ordered columnar phases of compounds **1** and **2** and the disordered columnar phase of compound **3**, the electron transport characteristics indicate a thermal- and field-activated hopping nature. The analysis of transport characteristics based on the one-dimensional Gaussian disorder model reveals large μ_0 values on the order of 10^0 cm^{2}V^{-1}s^{-1}, which is the reason that the LC-PTCBI derivatives exhibit high electron mobilities. For compound **1**, temperature-independent electron mobility is observed around room temperature between the two temperature regions. In spite of the bulkiness and liquid-like disordered structure of oligosiloxane chains, one-dimensional columnar aggregates of π-conjugated cores are constructed. The nanosegregated hybrid mesomorphic structures described in this study have the potential for creation of new soft materials with electronic functions.

Acknowledgements

Notes and references

[a] 2217-20 Hayashi-cho, Takamatsu, Kagawa 761-0396, Japan.

[b] 2217-14 Hayashi-cho, Takamatsu, Kagawa 761-0395, Japan.

Electronic Supplementary Information (ESI) available: [Synthetic procedure and spectral data of compound **2**, X-ray diffraction patterns and DSC thermograms of compounds **1-3**]. See DOI: 10.1039/b000000x/

1 (a) M. Kitamura, Y. Arakawa, *J. Phys. Condens. Matter*, 2008, **20**, 184011; (b) A. C. Grimsdale, K. L. Chan, R. E. Martin, P. G. Jokisz, A. B. Holms, *Chem. Rev.*, 2009, **109**, 897–1091; (c) C. Li, H. Wonneberger, *Adv. Mater.*, 2012, **24**, 623–636; (d) J. Roncali, *Acc. Chem. Res.*, 2009, **42**, 1719–1730; (e) J. Peet, A. J. Heeger, G. C. Bazan, *Acc. Chem. Res.*, 2009, **42**, 1700–1708; (f) K. Walzer, B. Maennig, M. Pfeiffer, K. Leo, *Chem. Rev.*, 2007, **107**, 1233–1271.

2 (a) A. Kim, K.-S. Jang, J. Kim, J. C. Won, M. H. Yi, H. Kim, D. K. Yoon, T. J. Shin, M.-H. Lee, J.-W. Ku, Y. H. Kim, *Adv. Mater.*, 2013, **25**, 6219–6225; (b) J. Lee, D. H. Kim, J.-K. Kim, B. Yoo, J. W. Chung, J. Park, B.-L. Lee, J. Y. Jung, J. S. Park, B. Koo, S. Im, J. W. Kim, B. Song, M.-H. Jung, J. E. Jang, Y. W. Jin, S.-Y. Lee, *Adv. Mater.*, 2013, **25**, 5886–5892.

3 (a) M. J. Hollambya, T. Nakanishi, *J. Mater. Chem. C*, 2013, **1**, 6178–6183; (b) J. E. Anthony, *Chem. Rev.*, 2006, **106**, 5028–5048.

4 (a) N. Boden, R. J. Bushby, J. Clements, M. V. Jesudason, P. F. Knowles, G. Williams, *Chem. Phys. Lett.*, 1988, **152**, 94–99; (b) N. Boden, R. J. Bushby, J. Clements, B. Movaghar, K. J. Donovan, T. Kreouzis, *Phys. Rev. B*, 1995, **52**, 13274–13280; (c) N. Boden, R. J. Bushby, J. Clements, *J. Chem. Phys.*, 1993, **98**, 5920–5931; (d) D. Adam, F. Closs, T. Frey, D. Funhoff, D. Haarer, H. Ringsdorf, P. Schuhmacher, K. Siemensmeyer, *Phys. Rev. Lett.*, 1993, **70**, 457–460; (e) A. M. van de Craats, J. M. Warman, K. Müllen, Y. Geerts, J. D. Brand, *Adv. Mater.*, 1998, **10**, 36–38; (f) A. M. van de Craats, J. M. Warman, A. Fechtenkötter, J. D. Brand, M. A. Harbison, K. Müllen, *Adv. Mater.*, 1999, **11**, 1469–1472; (g) H. Iino, Y. Takayashiki, J. Hanna, R. J. Bushby, D. Haarer, *Appl. Phys. Lett.*, 2005, **87**, 192105; (h) Y. Miyake, Y. Shiraiwa, K. Okada, H. Monobe, T. Hori, N. Yamasaki, H. Yoshida, M. J. Cook, A. Fujii, M. Ozaki, Y. Shimizu, *Appl. Phys. Exp.*, 2011, **4**, 021604; (i) M. Ichihara, A. Suzuki, K. Hatsusaka, K. Ohta, *Liq. Cryst.*, 2007, **34**, 555–567; (j) J. Kim, N. Yamasaki, T. Hayashi, M. Katayama, H. Yoshida, H. Moritake, A. Fujii, M. Ozaki, *Jpn. J. Appl. Phys.*, 2013, **52**, 101701.

5 (a) M. Funahashi, N. Tamaoki, *ChemPhysChem*, 2006, **7**, 1193–1197; (b) M. Funahashi, N. Tamaoki, *Chem. Mater.*, 2007, **19**, 608–617; (c) M. Nuita, J. Sakuda, Y. Hirai, M. Funahashi, T. Kato, *Chem.*

Lett., 2011, **40**, 412–413; (d) K. L. Woon, M. P. Aldred, P. Vlachos, G. H. Mehl, T. Stirner, S. M. Kelly, M. O'Neill, *Chem. Mater.*, 2006, **18**, 2311–2317; (e) K. Tokunaga, Y. Takayashiki, H. Iino, J. Hanna, *Phys. Rev. B*, 2009, **79**, 033201.

6 (a) M. Funahashi, J. Hanna, *Phys. Rev. Lett.*, 1997, **78**, 2184–2187; (b) M. Funahashi, J. Hanna, *Appl. Phys. Lett.*, 1997, **71**, 602–604; (c) M. Funahashi, J. Hanna, *Appl. Phys. Lett.*, 1998, **73**, 3733–3735; (d) M. Funahashi, J. Hanna, *Appl. Phys. Lett.*, 2000, **76**, 2574–2576; (e) M. Funahashi, J. Hanna, *Adv. Mater.*, 2005, **17**, 594–598. (f) K. Oikawa, H. Monobe, J. Takahashi, K. Tsuchiya, B. Heinrich, D. Guillon, Y. Shimizu, *Chem. Commun.*, 2005, 5337–5339.

7 (a) M. P. Aldred, A. E. A. Contoret, S. R. Farrar, S. M. Kelly, D. Mathieson, M. O'Neill, W. C. Tsoi, P. Vlachos, *Adv. Mater.*, 2005, **17**, 1368–1372; (b) T. Hassheider, S. A. Benning, H.-S. Kitzerow, M.-F. Achard, H. Bock, *Angew. Chem., Int. Ed. Engl.*, 2001, **40**, 2060–2063; (c) K. Kogo, T. Goda, M. Funahashi, J. Hanna, *Appl. Phys. Lett.*, 1998, **73**, 1595–1597; (d) M. W. Lauhof, S. A. Benning, H.-S. Kitzerow, V. Vill, F. Scheliga, E. Thorn-Csányi, *Synth. Met.*, 2007, **157**, 222–227; (e) S. A. Benning, R. Oesterhaus, H.-S. Kitzerow, *Liq. Cryst.*, 2004, **31**, 201–205.

8 (a) M. Funahashi, *Polym. J.*, 2009, **41**, 459–469; (b) M. Funahashi, F. Zhang, N. Tamaoki, *Adv. Mater.*, 2007, **19**, 353–358; (c) F. Zhang, M. Funahashi, N. Tamaoki, *Appl. Phys. Lett.*, 2007, **91**, 063515; (d) F. Zhang, M. Funahashi, N. Tamaoki, *Org. Electron.* 2010, **11**, 363–368; (e) H. Iino, J. Hanna, *Adv. Mater.*, 2011, **23**, 1748–1751; (f) A. J. J. M. van Breemen, P. T. Herwig, C. H. T. Chlon, J. Sweelssen, H. F. M. Schoo, S. Setayesh, W. M. Hardeman, C. A. Martin, D. M. de Leeuw, J. J. P. Valeton, C. W. M. Bastiaansen, D. J. Broer, A. R. Popa-Merticaru, S. C. J. Meskers, *J. Am. Chem. Soc.*, 2006, **128**, 2336–2345; (g) A. M. van de Craats, N. Stutzmann, O. Bunk, M. M. Nielsen, M. Watson, K. Müllen, H. D. Chanzy, H. Sirringhaus, R. Friend, *Adv. Mater.*, 2003, **15**, 495–499; (h) W. Pisula, A. Menon, M. Stepputat, I. Lieberwirth, U. Kolb, A. Tracz, H. Sirringhaus, T. Pakula, K. Müllen, *Adv. Mater.*, 2005, **17**, 684–689.

9 (a) T. Hori, Y. Miyake, N. Yamasaki, H. Yoshida, A. Fujii, Y. Shimizu, M. Ozaki, *Appl. Phys. Exp.*, 2010, **3**, 101602; (b) W. Shin, T. Yasuda, G. Watanabe, Y. S. Yang, C. Adachi, *Chem. Mater.*, 2013, **25**, 2549–2556.

10 (a) T. Kato, *Science*, 2002, **295**, 2414–2418; (b) T. Kato, N. Mizoshita, K. Kishimoto, *Angew. Chem., Int. Ed. Engl.*, 2006, **45**, 38–68; (c) F. J. M. Hoeben, P. Jonkheijm, E. W. Meijer, A. P. H. J. Schenning, *Chem. Rev.*, 2005, **105**, 1491–1546; (d) M. Yoneya, *Chem. Rec.*, 2011, **11**, 66–76; (e) B. Soberats, M. Yoshio, T. Ichikawa, S. Taguchi, H. Ohno, T. Kato, *J. Am. Chem. Soc.*, 2013, **135**, 15286–15289; (f) T. Ichikawa, M. Yoshio, S. Taguchi, J. Kagimoto, H. Ohno, T. Kato, *Chem. Sci.*, 2012, **3**, 2001–2008; (g) T. Yasuda, H. Ooi, J. Morita, Y. Akama, K. Minoura, M. Funahashi, T. Shimomura, T. Kato, *Adv. Funct. Mater.*, 2009, **19**, 411–419; (h) S. Yazaki, M. Funahashi, T. Kato, *J. Am. Chem. Soc.*, 2008, **130**, 13206–13207; (i) S. Yazaki, M. Funahashi, J. Kagimoto, H. Ohno, T. Kato, *J. Am. Chem. Soc.*, 2010, **132**, 7702–7708.

11 (a) G. H. Mehl, J. Goodby, *Angew. Chem., Int. Ed. Engl.*, 1996, **35**, 2641–2643; (b) I. M. Saez, J. W. Goodby, R. M. Richardson. *Chem. Eur. J.*, 2001, **7**, 2758–2764; (c) J. Newton, H. Coles, P. Hodge, J. Hannington, *J. Mater. Chem.*, 1994, **4**, 869–874; (d) J. C. Roberts, N. Kapernaum, F. Giesselmann, R. P. Lemieux, *J. Am. Chem. Soc.*,

This journal is © The Royal Society of Chemistry 2012

Phys. Chem. Chem. Phys., 2014, **00**, 1-3 | **9**

2008, **130**, 13842–13843; (e) D. Apreutesei, G. Mehl, *J. Mater. Chem.*, 2007, **17**, 4711–4715; (f) A. Zelcer, B. Donnio, C. Bourgogne, F. D. Cukiernik, D. Guillon, *Chem. Mater.*, 2007, **19**, 1992–2006.

12 (a) M. Funahashi, A. Sonoda, *Org. Electron.*, 2012, **13**, 1633–1640; (b) M. Funahashi, A. Sonoda, *J. Mater. Chem.*, 2012, **22**, 25190–25197; (c) M. Funahashi, A. Sonoda, *Dalton Trans.*, 2013, **42**, 15987–15994; (d) M. Funahashi, M. Yamaoka, K. Takenami, A. Sonoda, *J. Mater. Chem. C*, 2013, **1**, 7872–7878.

13 (a) I. Bleyl, C. Erdelen, H.-W. Schmidt, D. Haarer, *Philos. Mag. B*, 1999, **79**, 463–475; (b) H. Iino, J. Hanna, R. J. Bushby, B. Movaghar, B. J. Whitaker, *J. Appl. Phys.*, 2006, **100**, 043716; (c) L.-Y. Chen, F.-H. Chien, Y.-W. Liu, W. Zheng, C.-Y. Chiang, C.-Y. Hwang, C.-W. Ong, Y.-K. Lan, H. C. Yang, *Org. Electron.*, 2013, **14**, 2065-2070.

14 (a) X. Feng, V. Marcon, W. Pisula, M. R. Hanzen, J. Kirkpatrick, F. Grozema, D. Andrienko, K. Kremer, K. Müllen, *Nat. Mater.*, 2009, **8**, 421–426; (b) W. Pisula, M. Kastler, D. Wasserfallen, M. Mondeshki, J. Piris, I. Schnell, K. Müllen, *Chem. Mater.*, 2006, **18**, 3634–3640; (c) W. Pisula, X. Feng, K. Müllen, *Adv. Mater.*, 2010, **22**, 3634–3639.

15 (a) M. A. Palenberg, R. J. Silbey, M. Malagoli, J.-L. Brédas, *J. Chem. Phys.*, 2000, **112**, 1541–1546; (b) V. Duzhko, A. Semyonov, R. J. Twieg, K. D. Singer, *Phys. Rev. B*, 2006, **73**, 064201; (c) I. Shiyanovskaya, K. D. Singer, R. J. Twieg, L. Sukhomlimova, V. Gettwert, *Phys. Rev. E*, 2002, **65**, 041715; (d) T. Kreouzis, K. J. Donovan, N. Boden, R. J. Bushby, O. R. Lozman, Q. Liu, *J. Chem. Phys.*, 2001, **114**, 1797–1802.

16 (a) M. Funahashi, T. Ishii, A. Sonoda, *ChemPhysChem*, 2013, **14**, 2750–2758; (b) M. Funahashi, F. Zhang, N. Tamaoki, J. Hanna, *ChemPhysChem*, 2008, **9**, 1465–1473; (c) M. Funahashi, J. Hanna, *Mol. Cryst. Liq. Cryst.*, 2004, **410**, 529–540.; (d) A. Ohno, J. Hanna, *Appl. Phys. Lett.*, 2003, **82**, 751–753; (e) S. R. Farrar, A. E. A. Contoret, M. O'Neill, J. E. Nicholls, G. J. Richards, S. M. Kelly, *Phys. Rev. B*, 2002, **66**, 125107.

17 (a) R. G. Kepler, *Phys. Rev.*, 1960, **119**, 1226–1229; (b) W. E. Spear, *J. Non-Cryst. Solids*, 1968, **1**, 197–214.

18 (a) H. Bässler, *Phys. Status Solidi B*, 1993, **175**, 15–56; (b) A. Köhler, H. Bässler, *Top. Curr. Chem.*, 2012, **312**, 1–66; (c) R. Goehoorn, P. A. Bobbert, *Phys. Status Solidi A*, 2012, **209**, 2354–2377; (d) S. V. Novikov, D. H. Dunlap, V. M. Kenkre, P. E. Parris, A. V. Vannikov, *Phys. Rev. Lett.*, 1998, **81**, 4472–4475; (e) T. Nagase, K. Kishimoto, H. Naito, *J. Appl. Phys.*, 1999, **86**, 5026-5035.

19 (a) J. Pflaum, J. Niemax, A. K. Tripathi, *Chem. Phys.*, 2006, **325**, 152–159; (b) N. Karl, *Growth–Properties and Applications in Crystals*, ed. by H. C. Freyhardt, Springer Verlag, Berlin 1980.

10 | *Phys. Chem. Phys. Chem.*, 2014, **00**, 1-3

This journal is © The Royal Society of Chemistry 2012